

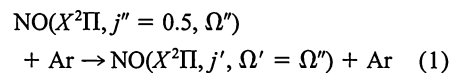
# Fully State-Resolved Differential Cross Sections for the Inelastic Scattering of the Open-Shell NO Molecule by Ar

Hiroshi Kohguchi,<sup>1</sup> Toshinori Suzuki,<sup>1,2\*</sup> Millard H. Alexander<sup>3</sup>

State-resolved differential cross sections (DCSs) for the inelastic scattering of  $\text{NO}(j'' = 0.5, \Omega'' = 1/2) + \text{Ar} \rightarrow \text{NO}(j', \Omega' = 1/2, 3/2) + \text{Ar}$  were obtained at a collision energy of  $516 \text{ cm}^{-1}$ , both experimentally and theoretically. A crossed molecular beam ion-imaging apparatus was used to measure DCSs for 20 final  $(j', \Omega')$  states, including spin-orbit conserving ( $\Delta\Omega = 0$ ) and changing ( $\Delta\Omega = 1$ ) transitions. Quantum close-coupling scattering calculations on ab initio coupled-cluster CCSD(T) and CEPA (correlated electron pair approximation) potential energy surfaces were also performed. Although small discrepancies were found for the  $\Delta\Omega = 1$  transitions, we find marked agreement between theory and experiment for the collision dynamics of this system, which is the paradigm for the collisional relaxation of a molecular radical.

Because of the large mass difference between electrons and nuclei, the coupling between the electronic and nuclear motion in a molecule is often ignored (the Born-Oppenheimer approximation). However, this so-called non-adiabatic coupling cannot be neglected whenever the spacing between electronic states becomes comparable to rovibrational spacings. This situation often occurs in collisions involving open-shell molecules with unpaired electrons. The effect of the breakdown of the Born-Oppenheimer approximation on molecular dynamics is an active focus of research.

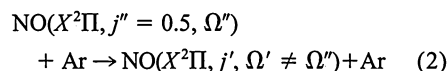
The rotationally inelastic scattering of the  $\text{NO}(X^2\Pi)$  molecule by Ar has emerged as the paradigm for nonadiabatic collisions of an open-shell molecule. Numerous experimental (1–8) and theoretical (9–13) studies of the Ar-NO system have been reported. The energy splitting between the  $\Omega = 1/2$  and  $3/2$  spin-orbit manifolds of the electronic ground state ( $^2\Pi$ ) of NO is only  $123 \text{ cm}^{-1}$  (14). Within each of these manifolds, there is a ladder of rotational levels characterized by a rotational constant of  $\sim 1.7 \text{ cm}^{-1}$ . Collision-induced transitions can occur between rotational levels associated with a given spin-orbit manifold:



and between levels associated with different spin-orbit manifolds:

<sup>1</sup>Institute for Molecular Science and Graduate University for Advanced Studies, Myodaiji, Okazaki 444-8585, Japan. <sup>2</sup>PRESTO, Japan Science and Technology Corporation, Japan. <sup>3</sup>Department of Chemistry and Biochemistry, University of Maryland, College Park, MD 20742-2021, USA.

\*To whom correspondence should be addressed. E-mail: suzuki@ims.ac.jp



State-resolved differential cross sections (DCSs) under well-defined collision conditions are the most sensitive probe of collision dynamics (15). The correct framework for exact quantum scattering calculations for the open-shell NO + Ar system was established in the early 1980s (16). However, accurate theoretical predictions were hindered by the inaccuracy of the available potential energy surfaces (PESs), which were determined first within the electron-gas model (17) and later from ab initio CEPA (correlated electron pair approximation) (13). Also, the accuracy and completeness of earlier experimental studies have not been sufficient to provide a definitive measurement of the complex oscillatory structures in the DCSs, which are sensitive functions of the final-state quantum numbers  $(j', \Omega')$ . In addition, there have been no previous experimental determinations of state-resolved DCSs for the spin-orbit changing transitions, which are a direct probe of nonadiabaticity in the collision but which are considerably smaller in magnitude than the DCSs for spin-orbit conserving transitions.

We now report state-to-state DCSs for both spin-orbit conserving and changing transitions observed by high-resolution ion-imaging in a crossed molecular beam apparatus at a collision energy of  $516 \text{ cm}^{-1}$ . The experimental DCSs are compared with quantum-scattering calculations based on the ab initio CEPA (13) and the recent coupled-cluster CCSD(T) PESs (10). The latter is the most accurate Ar-NO PES available at present.

The details of the crossed beam appara-

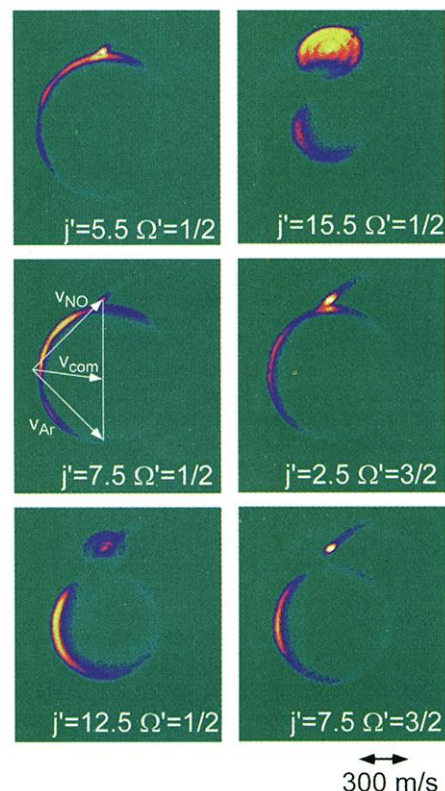


**Fig. 1.** Examples of observed images for the inelastic scattering of  $\text{NO}(j'' = 0.5, \Omega'' = 1/2) + \text{Ar} \rightarrow \text{NO}(j', \Omega' = 1/2, 3/2) + \text{Ar}$  at a collision energy of  $516 \text{ cm}^{-1}$ . The final states are labeled by  $(j', \Omega')$  on each image. The  $(j' = 5.5, \Omega' = 1/2)$  and  $(j' = 2.5, \Omega' = 3/2)$  states were observed without discrimination of the  $\Lambda$ -doublet level (*e*- and *f*-state). The *f*-state was selectively observed for all of the other states. A Newton diagram is superimposed in the image of  $(j' = 7.5, \Omega' = 1/2)$ , where the collision axis is configured vertically. The spot at the end the  $\mathbf{v}_{\text{NO}}$  vector is an ion signal from rotationally warm, unscattered NO in the incident beam.

tus have been described elsewhere (18–20). The NO rotational temperature was 3 K, so that about 90% of the NO in the beam is in its lowest quantum state,  $(j = 0.5, \Omega = 1/2)$ , with equal population of the two  $\Lambda$ -doublet (*e/f*) levels. The collision energy between NO and Ar was  $516 \text{ cm}^{-1}$  with full-width at half-maximum (FWHM) of  $56 \text{ cm}^{-1}$ .

These velocity-mapped images (Fig. 1) show directly the velocities of the scattered NO (21), with the exception of small spots due to thermally excited NO molecules in the primary beam that move with the NO beam velocity. Twenty  $(j', \Omega')$  states, including 11 spin-orbit conserving ( $\Delta\Omega = 0$ ) transitions and 9 spin-orbit changing ( $\Delta\Omega = 1$ ) transitions, were observed. The asymmetry of observed images about the collision axis shows that they are strongly influenced by the angle-dependent product detection efficiency. The DCSs were extracted from these observed images by a simulation that took into account the temporal

**Fig. 2.** State-resolved DCSs for the inelastic,  $\Omega$  conserving, scattering of  $\text{NO}(j'' = 0.5, \Omega'' = 1/2) + \text{Ar} \rightarrow \text{NO}(j', \Omega' = 1/2) + \text{Ar}$  at a nominal collision energy of  $516 \text{ cm}^{-1}$ . The final states are labeled by  $(j', \Omega', e, \text{ or } f)$  on each graph. The transitions for which the final  $\Lambda$ -doublet was not resolved are denoted by  $e/f$ . The black lines represent the experimental differential cross sections. The red and blue lines are the theoretical results based on the CCSD(T) and the CEPA ab initio PESs, respectively. The DCS are normalized so that the integrated DCSs, both experimental and theoretical, have the same value in all of the subplots. The theoretical DCSs are averaged over the  $\Lambda$ -doublet levels of the initial ( $j'' = 0.5, \Omega'' = 1/2$ ) state and then smoothed to simulate the experiment, first over a Gaussian distribution in collision energy with  $56 \text{ cm}^{-1}$  (FWHM), then convoluted over a Gaussian angular window of  $8^\circ$  (FWHM).

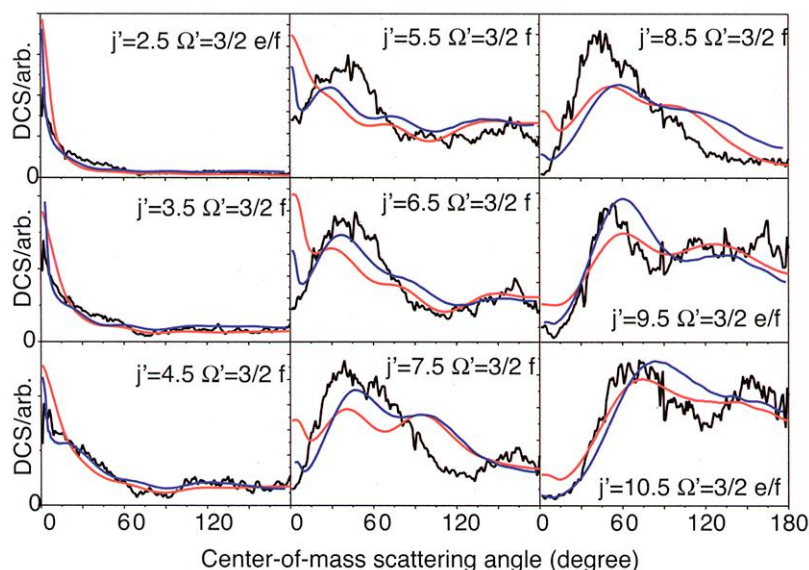
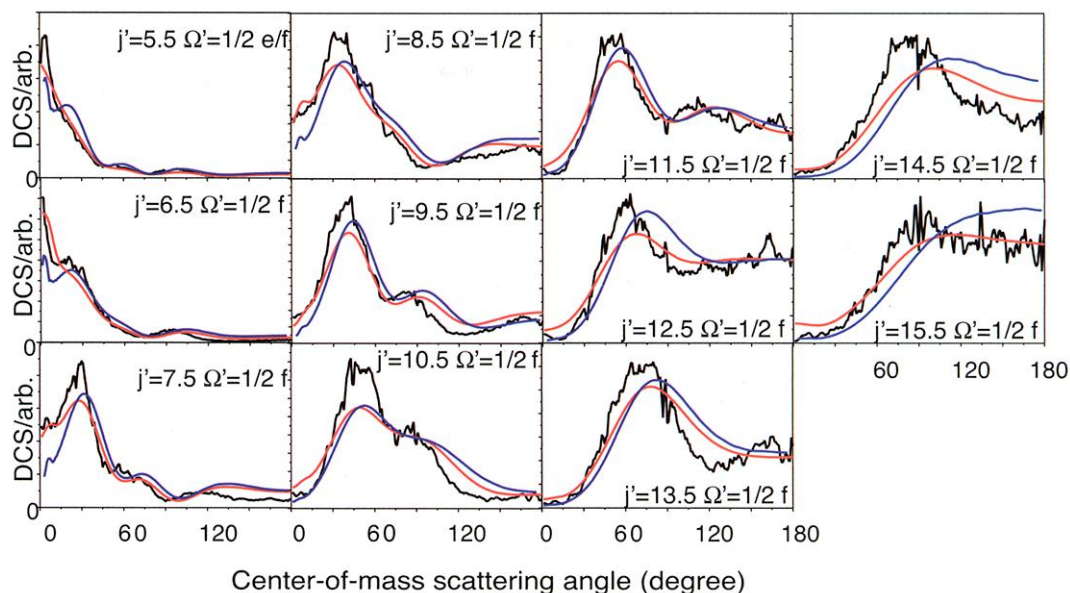


**Fig. 3.** State-resolved DCSs for the inelastic scattering of  $\text{NO}(j'' = 0.5, \Omega'' = 1/2) + \text{Ar} \rightarrow \text{NO}(j', \Omega' = 3/2) + \text{Ar}$  with the collision energy of  $516 \text{ cm}^{-1}$  (the  $\Delta\Omega = 1$  transitions). The detailed legend for these plots is identical to that of Fig. 2.

overlap of the pulsed molecular beams (22).

The noncollinear approach of the Ar atom lifts the degeneracy of the  $X^2\Pi$  state of NO in a manner equivalent to the Renner-Teller effect in triatomic molecules (23, 24). The relevant two electronically adiabatic PESs are designated by the electronic symmetry of the wave functions,  $A'$  and  $A''$  (in  $C_s$  geometry) (9). Inelastic collisions sample both PESs equally. In the theoretical treatments, it is necessary to transform the  $A'$  and  $A''$  surfaces to sum ( $V_{\text{sum}}$ ) and difference ( $V_{\text{diff}}$ ) PESs (9). In the Hund's case (a) limit,  $V_{\text{sum}}$  and  $V_{\text{diff}}$  are responsible, separately, for the  $\Delta\Omega = 0$  and

$\Delta\Omega = 1$  transitions (10, 16). The most important difference between the CEPA and CCSD(T) PESs is that the wells in both in the  $A'$  and the  $A''$  CCSD(T) PESs are deeper than those predicted by the CEPA calculations (10, 25).

Full quantum close-coupling calculations, without any dynamical approximations and based on the CEPA and the CCSD(T) PESs, were performed with the HIBRIDON 4.1 program suite (26). DCSs for the scattering of NO from an initial ( $j'', \Omega'', \epsilon''$ ) state to a final ( $j', \Omega', \epsilon'$ ) state, summed over the projection quantum numbers of the final rotational state and aver-

aged over the projection quantum numbers of the initial rotational state, were obtained from the fundamental scattering amplitude. The parity index  $\epsilon$  designates the  $e$  ( $\epsilon = +1$ ) or  $f$  ( $\epsilon = -1$ )  $\Lambda$ -doublet levels. Only the  $v = 0$  vibrational levels of NO were included in the channel expansion because the collision energy of our experiments did not allow vibrational excitation [ $\omega_e = 1904 \text{ cm}^{-1}$  (14)]. For comparison with experiment, the calculated DCSs were convoluted over Gaussian distributions in collision energy and angle typical of the experimental conditions and averaged over the unselected  $\Lambda$ -doublet levels of the initial state.

The experimental DCSs vary substantially with the final ( $j', \Omega'$ ) state. For the  $\Delta\Omega = 0$  transitions into  $j' = 5.5$  and  $6.5$ , the DCSs in Fig. 2 show forward peaks around  $\theta_{\text{cm}}$  (center-of-mass scattering angle)  $= 0^\circ$ . Undulations with a period of  $\sim 30^\circ$  are seen in both cases. For scattering into the  $j' = 7.5$  to  $10.5$  states, the maximum in the DCS shifts progressively to larger scattering angles as  $j'$  increases. Transitions into states with  $j'$  higher than  $11.5$  show substantial backward scattering intensity ( $\theta_{\text{cm}} = 180^\circ$ ). By contrast, in these cases the forward intensity ( $\theta_{\text{cm}} = 0^\circ$ ) decreases almost to zero.

For the spin-orbit changing ( $\Delta\Omega = 1$ ) transitions shown in Fig. 3, we observe considerable variation in the scattering as a function of  $j'$ . We find a sharp forward peak for the  $j' = 2.5$  to  $4.5$  transitions. The undulations are not as pronounced as for the  $\Delta\Omega = 0$  transitions. The DCSs for transitions into  $j'$  states higher than  $5.5$  do not show a forward peak. Broad undulations with a period of several tens of degrees, or two broad peaks, are seen for the

$j' = 5.5$  to  $7.5$  states. The intensity at  $\theta_{\text{cm}} = 0^\circ$  drops for the  $j'$  states higher than  $6.5$ . The DCSs for the  $j' = 9.5$  and  $10.5$  states show substantial backward intensity.

As seen in Figs. 2 and 3, the theoretical predictions based on the CEPA and the CCSD(T) PESs are in good agreement with experiment, although the high resolution achieved in the present experiment reveals a slightly better agreement with the CCSD(T) predictions. For the  $\Delta\Omega = 0$  transitions (Fig. 2), the position and period of the observed undulations are reproduced almost exactly. Because the close-coupling calculations are free of approximation and converged, any inaccuracies in the theoretical predictions are the result of inaccuracies in the ab initio PESs used. Careful comparison of the theoretical DCSs reveals how the slight differences between the CEPA and the CCSD(T) PESs manifest themselves in the state-resolved DCSs. The major differences between the DCSs predicted by these two PESs are found primarily in the forward direction. The sharp forward peak predicted by both the CEPA and CCSD(T) surfaces is also seen in the experimental DCSs for the  $(j', \Omega') = (5.5, 1/2)$ ,  $(6.5, 1/2)$ ,  $(2.5, 3/2)$ ,  $(3.5, 3/2)$ , and  $(4.5, 3/2)$  states. However, for the nonadiabatic  $\Omega$ -changing transitions, noticeable disagreement between both the theoretical and the experimental results occurs in the forward directions for intermediate  $j'$  states ( $5.5$  to  $8.5$ ). Here the CCSD(T) DCSs are substantially larger (relative to other scattering angles) than seen experimentally.

Unfortunately, it is not totally clear yet which region(s) of the PES are most responsible for this discrepancy. The DCSs for the  $\Delta\Omega = 1$  transitions are expected to be sensitive to the anisotropy of  $V_{\text{diff}}$  around the classical turning point where the potential will be steeply rising. The accurate determination of the short-ranged, highly anisotropic  $V_{\text{diff}}$  is difficult because this PES represents the small difference between the  $A'$  and  $A''$  PESs, which are already quite similar to each other. In contrast, in collisions of a close-shell species, forward scattering is due predominantly to the long-range, attractive part of the PES (27).

The most notable result of the present experiments is the slowly varying undulations in the DCS found for almost all the observed transitions. The width of these undulations and their shift to higher angle as the rotational inelasticity increases are markedly similar to those earlier predicted for the scattering of  $\text{Na}_2$  by He (28). In this work, the undulatory structure was shown to be a manifestation of the ellipsoidal nature of any atom-molecule PES. Also, in principle, the forward peaks should be overlaid by fast oscillations with a period of several degrees, which correspond to supernumerary rainbows. However, the collision energy spread (10%) in our crossed beam ex-

periment precludes observation of this feature. Forward scattering involves interference of a large number of partial waves, which results in fast oscillation, whereas a relatively limited number of partial waves contribute to the sideways or backward scattering. Thus, we can observe the slow undulations in the present experiments even with a finite collision energy spread.

The detailed structures in the observed state-resolved DCSs obtained by our high-resolution ion-imaging are quantum features reproducible only by rigorous quantum scattering calculations. Both the  $V_{\text{sum}}$  and  $V_{\text{diff}}$  PESs contribute to spin-orbit changing collisions. Consequently, these are nonadiabatic processes, which cannot be described by conventional classical trajectory calculations on a single PES. The present comparison demonstrates that quantum scattering calculations are now sufficiently accurate to describe the fine details of DCSs for collisions involving open-shell molecules.

As an incentive to future work, we point out, first, that the ab initio calculations described in (10) and (13) were based on the assumption that the NO molecule could be fixed at its equilibrium internuclear distance without loss of accuracy. Recent calculations on the Al-H<sub>2</sub> van der Waals molecule (29) have shown that inclusion of the dependence of the PESs on the intramolecular stretch coordinate ( $r_{\text{H-H}}$ ) results in substantially (~20%) deeper wells and a near quantitative agreement with the results of spectroscopic experiments, even though the first vibrationally excited state is inaccessible [ $\omega_e(\text{H}_2) = 4395 \text{ cm}^{-1}$  (14)], as is the case here. It may well be that the differences seen here between the calculated and experimental DCSs for the spin-orbit changing transitions would be reduced if the PES calculations were extended to include the dependence on the NO bond distance. Concurrently, additional effort should be devoted to improving the accuracy and precision of the experimental DCSs and to obtaining the relative (or, better, the absolute) magnitude of the DCSs associated with the various inelastic transitions probed here.

#### References and Notes

- P. Andresen, H. Joswig, H. Pauly, R. Schinke, *J. Chem. Phys.* **77**, 2204 (1982).
- K. T. Lorenz *et al.*, *Science* **293**, 2063 (2001).
- C. R. Bieler, A. Sanov, H. Reisler, *Chem. Phys. Lett.* **235**, 175 (1995).
- A. Lin, S. Antonova, A. P. Tsakotellis, G. C. McBane, *J. Phys. Chem. A* **103**, 1198 (1999).
- S. D. Jons, J. E. Shirley, M. T. Vonk, C. F. Giese, W. R. Gentry, *J. Chem. Phys.* **105**, 5397 (1996).
- L. S. Bontuyan, A. G. Suits, P. L. Houston, B. J. Whitaker, *J. Phys. Chem.* **97**, 6342 (1993).
- M. J. L. de Lange *et al.*, *Chem. Phys. Lett.* **313**, 491 (1999).
- Y. Kim, K. Patton, J. Fleniken, H. Meyer, *Chem. Phys. Lett.* **318**, 522 (2000).
- M. H. Alexander, *Chem. Phys.* **92**, 337 (1985).
- \_\_\_\_\_, *J. Chem. Phys.* **111**, 7426 (1999).
- T. Orlikowski, M. H. Alexander, *J. Chem. Phys.* **79**, 6006 (1983).

- G. C. Corey, M. H. Alexander, *J. Chem. Phys.* **85**, 5652 (1986).
- M. H. Alexander, *J. Chem. Phys.* **99**, 7725 (1993).
- G. Herzberg, *Molecular Spectra and Molecular Structure. I. Spectra of Diatomic Molecules* (Princeton Univ. Press, Princeton, NJ, 1968).
- H. E. van den Bergh, M. Faubel, J. P. Toennies, *Faraday Disc. Chem. Soc.* **55**, 203 (1973).
- M. H. Alexander, *J. Chem. Phys.* **76**, 5974 (1982).
- G. C. Nielson, G. A. Parker, R. T. Pack, *J. Chem. Phys.* **66**, 1396 (1977).
- N. Yonekura, C. Gebauer, H. Kohguchi, T. Suzuki, *Rev. Sci. Instrum.* **70**, 3265 (1999).
- T. Suzuki, *Faraday Disc. Chem. Soc.* **113**, 485 (1999).
- Two supersonic jets with stagnation pressures of 3 atm were skimmed 45 mm downstream from the orifice to generate molecular beams 2 mm in diameter. These two beams were crossed 95 mm downstream from the nozzle.
- The scattered NO was ionized by [1+1] resonantly enhanced multiphoton ionization via the  $A^2\Sigma^+ - X^2\Pi$ ,  $v'-v'' = 0-0$  band around 226 nm. The wavelength of the probe laser was tuned to individual rotational lines to observe the state-resolved DCSs. R branches were used to detect a single  $\Lambda$ -doublet level (the  $f$ -state in this case) of each final  $(j', \Omega')$  state. The ionized NO molecules were accelerated by an electric field toward a microchannel plate (MCP), while the velocity components parallel to the detector plane were unaffected. A light spot due to each ion impact on the phosphor screen behind the MCP was captured by an intensified charge-coupled device camera and accumulated by a computer.
- Accurate estimation of the errors in the extracted DCSs is extremely difficult. To do so, we carried out simulations of the ion images with reasonable variations of the experimental parameters. We estimate the angular resolution to be  $8^\circ$  and the relative accuracy of the DCSs as a function of scattering angle to be  $\pm 10\%$  for strong transitions. The uncertainty in DCS is larger than 10% for weak transitions. Supplemental text describing the details of the data analysis and error evaluation is available on Science Online at [www.sciencemag.org/cgi/content/full/294/5543/832/DC1](http://www.sciencemag.org/cgi/content/full/294/5543/832/DC1).
- J. M. Brown, F. Jørgensen, *Adv. Chem. Phys.* **52**, (1983).
- R. G. Macdonald, K. Liu, *J. Chem. Phys.* **91**, 821 (1990).
- In both ab initio calculations, the  $A'$  PES has a minimum at  $\theta \sim 95^\circ$ , whereas the  $A''$  PES has its minimum at  $\theta \sim 70^\circ$  with a broader well. The well depths in the CCSD(T) PESs are  $D_e(A') = 115.9 \text{ cm}^{-1}$  and  $D_e(A'') = 111.0 \text{ cm}^{-1}$ , and those in the CEPA PESs are  $D_e(A') = 77.9 \text{ cm}^{-1}$  and  $D_e(A'') = 79.1 \text{ cm}^{-1}$ .
- HIBRIDON is a program suite for the time-independent quantum treatment of inelastic collisions and photodissociation written by M. H. Alexander, D. E. Manolopoulos, H.-J. Werner, and B. Follmeg, with contributions by P. F. Vohralik, D. Lemoine, G. Corey, B. Johnson, T. Orlikowski, W. Keaney, A. Berning, A. Degli-Esposti, C. Rist, and P. Dagdigan.
- R. D. Levine, R. B. Bernstein, *Molecular Reaction Dynamics and Chemical Reactivity* (Oxford Univ. Press, New York, 1987).
- H. J. Korsch, R. Schinke, *J. Chem. Phys.* **75**, 3850 (1981).
- X. Tan, P. J. Dagdigan, J. Williams, M. H. Alexander, *J. Chem. Phys.* **114**, 8938 (2001).
- The experimental work at Okazaki was supported by a Grant-in-Aid from the Ministry of Education, Culture, Sports, Science and Technology of Japan (09440208 and 09044110). T.S. gratefully acknowledges financial support from NEDO (New Energy and Industrial Technology Development Organization) in the early stages of this project. M.H.A. thanks the U.S. National Science Foundation for support of the theoretical work at Maryland under grant CHE-9971810. We dedicate this paper to the memory of the late Professor Peter Andresen, who pioneered the study of the rotationally inelastic scattering of open-shell systems.

25 June 2001; accepted 25 September 2001